Hindawi
Scientific Programming
Volume 2021, Article ID 6246274, 7 pages
https://doi.org/10.1155/2021/6246274

Research Article

Prediction and Value of Ultrasound Image in Diagnosis of Fetal Central Nervous System Malformation under Deep Learning Algorithm

Yuehong Zhou

Department of Ultrasound Imaging, Suizhou Central Hospital, Suizhou 441300, Hubei, China

Correspondence should be addressed to Yuehong Zhou; zhouyuehong@cumt.edu.cn

Received 10 May 2021; Revised 29 June 2021; Accepted 16 July 2021; Published 27 July 2021

Academic Editor: Gustavo Ramirez

Copyright © 2021 Yuehong Zhou. This is an open access article distributed under the Creative Commons Attribution License, which permits unrestricted use, distribution, and reproduction in any medium, provided the original work is properly cited.

This study was to explore the application of deep learning neural network (DLNN) algorithms to identify and optimize the ultrasound image so as to analyze the effect and value in diagnosis of fetal central nervous system malformation (CNSM). 63 pregnant women who were gated in the hospital were suspected of being fetal CNSM and were selected as the research objects. The ultrasound images were reserved in duplicate, and one group was defined as the control group without any processing, and images in the experimental group were processed with the convolutional neural network (CNN) algorithm to identify and optimize. The ultrasound examination results and the pathological test results before, during, and after the pregnancy were observed and compared. The results showed that the test results in the experimental group were closer to the postpartum ultrasound and the results of the pathological result, but the results in both groups showed no statistical difference in contrast to the postpartum results in terms of similarity ($P > 0.05$). In the same pregnancy stage, the ultrasound examination results of the experimental group were higher than those in the control group, and the contrast was statistically significant ($P < 0.05$); in the different pregnancy stages, the ultrasound examination results in the second trimester were more close to the postpartum examination results, showing statistically obvious difference ($P < 0.05$). In conclusion, ultrasonic image based on deep learning was higher in CNSM inspection; and ultrasonic technology had to be improved for the examination in different pregnancy stages, and the accuracy of the examination results is improved. However, the amount of data in this study was too small, so the representative was not high enough, which would be improved.

1. Introduction

With the rapid development of society, the economic level is getting better and better, the national fertility policy is also relaxed, and the fertility rate of the second child also increases. However, neonatal mortality and disability are also increasing, which are caused by many reasons, among which the central nervous system malformation (CNSM) is one of the important reasons. CNSM is one of the most common types of fetal malformations in the mother [1]. In addition, the number of elderly pregnant women increases with the opening of the two-child policy, leading to a higher and higher incidence of CNSM. At present, prenatal ultrasound examination is the most important and widely accepted method for prenatal screening of fetal CNSM [2]. It is a noninvasive examination with simple operation process, so it is a convenient and effective examination method for pregnant women. It can directly display the fetal skull structure and can conduct a better identification examination for the fetus with CNSM [3]. The best time for examination is the second trimester, which is recognized and proposed by the International Society of Ultrasound in Obstetrics and Gynaecology [4]. However, as the structure of the fetal nervous system is too complex and CNSM is a common type of fetal malformations, its causes are various, and the types of malformations are also diverse. Thus, the ultrasound reflection is different, leading to a large difference in ultrasound examination in the middle of pregnancy, which is very unfavorable for the early time of the fetus [4]. Therefore, how to realize an accurate and effective diagnosis

of the CNSM of the fetus earlier becomes the focus of the current research study [5].

With the progress of science and technology, the deep learning in the category of artificial intelligence has been greatly developed and extensively used. In the medical field, imaging technology is used to process medical images and achieves good results. At this stage, the neural network algorithm of deep learning is one of the most practical learning algorithms [6]. The depth learning method has been widely used in medical image identification, detection, and segmentation.

In this study, the DLNN algorithm was adopted to process the ultrasound images of the fetus with CNSM and to analyze its value in diagnosis of fetal CNSM. 63 pregnant women of suspected fetal CNSM were selected as the research subjects. It was expected to provide a theoretical basis for the treatment of CNSM.

2. Materials and Methods

2.1. Research Objects. 63 pregnant women who were admitted to Suizhou Central Hospital from January 2018 to February 2020 were selected as the research subjects. They had clinical symptoms but were not diagnosed with CNSM. The pregnant women were 25~39 years old, with an average age of 28.3 ± 4.9. There were 43 primiparas and 20 multiparas; the pregnancy cycle was 17 to 32 weeks, with the average cycle of 24.1 ± 3.1 weeks; and all pregnant women were single tires. The included criteria were defined as follows: the pregnant women who were aged over 18 years old and less than 40 years old; pregnant women who were pregnant for single tires; pregnant women with ultrasound inspection within 17 weeks to 32 weeks; pregnant women who were able to communicate smoothly and without mental illness; and pregnant women who signed the informed consents. The excluded criteria were defined as follows: pregnant women who suffered from the central nervous system; pregnant woman who failed to participate the complete research process; pregnant women with serious malfunction in heart, liver, kidney, and other organs; and pregnant women who suffered from large bleeding in the vagina and acute fetal endo. This study was approved by the ethics committee of the hospital, and all the subjects who were included into the study signed the informed consent form.

2.2. Examinations and Grouping. All pregnant women were tested using the voluson-e8 ultrasonic detector under the guidance of the same professional doctors. The continuous scanning was performed under the guidance of the *Prenatal Ultrasound and Ultrasound Inspection Guide*, and the specific scanning site is shown in Table 1. The ultrasound images were reserved in duplicate, and one group was defined as the control group without any processing, and images in the experimental group were processed with the CNN algorithm to identify and optimize. The results of ultrasound examination and other clinical inspections were informed to the pregnant women, who had to decide whether to continue the pregnancy or immediately terminate the pregnancy. For pregnant women who continued to pregnancy, the fetus had to be repeatedly examined after childbirth; for pregnant women who terminated the pregnancy, the CNSM would be diagnosed based on the pathological results of the fetus. The diagnosis value and effect of ultrasound image based on the depth learning algorithm were analyzed by comparing the ultrasound examination results before and after the birth with the pathological test results.

2.3. Establishment of Ultrasonic Image Denoising Model Based on CNN Algorithm. CNN is mainly composed of a convolutional layer, a pooling layer, and a full connection layer. With the continuous progress of science and technology, CNN has been improved into the structure composed of a convolutional layer, a pooling layer, a full connection layer, and a deconvolution layer [7].

The Java Fuzzy Cognitive Maps (JFCM) algorithm is used to filter the features. In this process, the preclassification is screened to improve the accuracy of classification results. The standard selection is shown the following equation:

$$\frac{F\left(w_{\varphi o} \in D_{ij} \wedge \Omega_{\varphi o} = \Omega_{ij}\right)}{n \times n} > \kappa. \tag{1}$$

In equation (1), (I, j) referred to the position of the feature map, Ω_{ij} referred to the mark of pixel p_{ij}, and $n \times n$ is the size of the feature map.

The 1^{th} layer was assumed as the convolution layer, and the feature map of the ultrasonic detection image was inputted in the $l-1^{\text{th}}$ layer, which can be expressed as the following equation:

$$M(h, p) = \sum_{b=1}^{B} X^{(h,p,b)} \otimes N^{(h-1,b)} + j^{(h,p)}. \tag{2}$$

In equation (2), $X^{(h,p,b)}$ represents the convolution kernel, $j^{(h,p)}$ refers to the bias, and b represents the number of feature graphs.

To enable the network computing process to increase the ability to express data characteristics, some experts have proposed nonlinear activation function [8]. In this study, a relatively common and fast ReLU function is used as an activation function, which can be expressed as equation (2), and the corresponding derivative function can be represented as shown in the following equation:

$$\begin{aligned} f(x) &= \max(0, x), \\ f'(x) &= \begin{cases} x, & x > 0, \\ 0, & x \le 0. \end{cases} \end{aligned} \tag{3}$$

The ultrasonic image map for the fetal central nervous system is set as H. All pixels in the image H are expressed as T and the set form of which is $(t_1, t_2, \ldots, t_n)$. The image portion that needs to be identified is expressed by U, which can be $(u_1, u_2, \ldots, u_n)$, and then the probability of the pixel S_n of the j^{th} channel corresponding to the output u_j is as follows:

Table 1: Scanning sites at different pregnancy stages.

Pregnancy stages	The first trimester (17~19 weeks)	Second trimester (20~33 weeks)
Scanning site	The uterus and adnexa uteri of pregnant women; the head hip long, double top diameter, femur long, neck transparent belt thickness and nasal bone, and tibia length of fetus; and the malformation of brain, bones, cardiovascular, nerve, and urology	The uterus and adnexa uteri of pregnant women; basic conditions of fetus, such as head hip long, double top diameter, head circumference, and femur diameter; the abnormal structure of fetal limbs, internal organs, and face; the spine, skull, intracranial structure (cerebellum, thalamus, posterior fossa cistern, cerebral line, ventricle, and choroid plexus) along the spine long axis, cerebellum, and postcranial pool, sagittal head chest, and side cerebral chamber

$$p\left(t_n = u_j\right) = \frac{1}{E}\exp\left[v\left(u_j\right)\right]. \tag{4}$$

In equation (4), $v(u_j)$ refers to the value of u_j, E is the regularization, and the predicted value y_n of S_n can be expressed as $y_n = \arg\max[p(s_n = u_j)]$, and the corresponding loss function can be written as follows:

$$L = -\frac{1}{cd}\sum_n \sum_j y_{nj} \ln\left[p\left(s_n = u_j\right)\right]. \tag{5}$$

Standardization batch normalization (BN) is one of the methods of optimizing the neural network. It can reduce the learning difficulty, allowing us to get rapid improvement in the exercise model. The method is to process the previous step in advance when each layer is processed to standardize the data [9]. It was used to improve the CNN-based algorithm in this study.

The expression equation of BN is given as follows:

$$\overline{Y}^i = \frac{Y^{(i)} - Z\left[Y^i\right]}{\sqrt{\mathrm{Var}\left[Y^{(i)}\right]}}. \tag{6}$$

In equation (6), $Z[Y^i]$ refers to the average value of $Y^{(i)}$ in each group of samples and $\mathrm{Var}[Y^{(i)}]$ refers to the variance. However, there are some problems for equation (5), so the new parameters β and μ are introduced in equation (6), and then the new expression equation of BN is given as follows:

$$\begin{aligned} Q^i &= \beta^{(i)}\overline{Y}^{(i)} + \mu^{(i)}, \\ \beta^{(i)} &= \sqrt{\mathrm{Var}\left[Y^{(i)}\right]}, \\ \mu^{(i)} &= Z\left[Y^i\right], \\ Z &= \frac{\beta}{\sqrt{\mathrm{Var}[Y] + \varphi}} \cdot X + \left(\mu - \frac{\beta Z(Y)}{\sqrt{\mathrm{Var}[Y] + \varphi}}\right). \end{aligned} \tag{7}$$

BN is a single layer, which is placed behind the convolution layer and in front of the activation function.

After the convolution processing of the CNN algorithm, the ultrasonic image with the size of 465 ∗ 393 is obtained from the feature image with the size of 223 ∗ 224. After multiple deconvolution processing, the information reflected in the feature image is clearer, as shown in Figure 1.

The following two methods are adopted to evaluate whether the results obtained after the CNN algorithm processing are ideal and effective after the ultrasound image processing is completed.

One method is dice similar coefficient (DSC), which refers to the overlapping extent between the area divided by radiologist and the area divided by PSSNET, and the calculation equation is shown in the following equation:

$$\mathrm{DSC} = \frac{2|Q \cap W|}{|Q| + |W|}. \tag{8}$$

In equation (8), Q refers to the standard region value segmented by the radiologist and W refers to the result region segmented by the CNN model. The range of DSC is set as [0,1]. When it is the minimum value 0, there is no overlap between Q and W; on the contrary, when it meets the maximum value 1, Q and W are perfectly overlapping. This indicates that the larger the DSC value is obtained, the higher the coincidence degree of QW will be and the better the segmentation result will be.

The other method is Hausdroff distance (HD), which refers to the maximum range of mismatches between two sets of numbers, and it is used to evaluate the degree of similarity between two sets of numbers.

The point in the ultrasound image of group M could be set to $Q = \{q_1, q_2, q_3, \ldots, q_x\}$, and that in group W can be defined as $W = \{w_1, w_2, w_3, \ldots, w_x\}$, and then the following equations are obtained:

$$\begin{aligned} \mathrm{HD}(Q, W) &= \max(h(Q, W), h(Q, W)), \\ h(Q, W) &= \max(q \in Q)\min(w \in W)\|q - w\|, \\ h(Q, W) &= \max(w \in W)\min(q \in Q)\|w - q\|. \end{aligned} \tag{9}$$

The smaller the value of HD is, the higher the similarity is and the higher the medium overlap degree of the image is. In other words, when $Q = W$, the result is the most ideal.

2.4. Statistical Methods. SPSS22.0 software was used for statistical analysis of the result data. The count data were expressed as n (%), and χ^2 test was used. The measurement data were expressed as (x), and the t-test was used. $P < 0.05$ indicated that the difference was statistically significant.

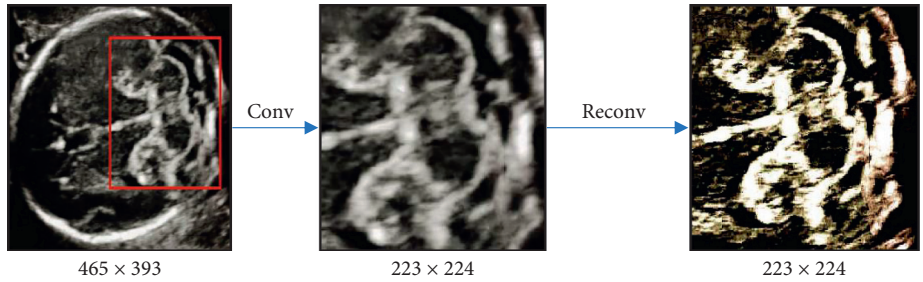

Figure 1: Ultrasound image processing of the fetal central nervous system.

3. Results

3.1. Comparison of Central Nervous System Ultrasound Images between Two Groups of Normal Fetuses. The ultrasound images of coronal section and lateral paraventricular sagittal section of normal fetal brain before and after treatment in the two groups (as shown in Figures 2 and 3) showed that the images after treatment (the experimental group) were more specific and more prominent than those before treatment (the control group).

3.2. Comparison between the Prenatal and Postpartum CNN-Based Ultrasound Diagnosis Results and the Pathological Results. Table 2 shows the statistics of prenatal CNN-based ultrasound diagnosis results and postpartum ultrasound examination results or pathological tissue biopsy test results. The data revealed that the test results in the experimental group were more close to the postpartum ultrasound and the results of the pathological result, but the results in both groups showed no statistical difference in contrast to the postpartum results in terms of similarity ($P > 0.05$), as shown in Figure 4.

3.3. Comparison of Prenatal and Postnatal Ultrasound and Pathological Examination Results at Different Pregnancy Stages. Table 3 shows the results of ultrasound examinations in the first trimester and the second trimester pregnancy stage as well as the postpartum ultrasound and pathological examination results of pregnant women in the control group and the experimental group. The observation and analysis results revealed that the similarities between the ultrasound examination results of the first trimester and the postpartum ultrasound and pathological examination results were the 33.3%(control group) and 63.5% (experimental group), respectively, while those in the second trimester were 63.5% (control group) and 82.5% (experimental group), respectively. Thereby, the results of ultrasound examination in the experimental group were higher than those in the control group in both the first trimester and late pregnancy, showing statistically observable difference ($P < 0.05$), as shown in Figure 5. In addition, the similarity between the ultrasound examination results and the postpartum ultrasound and pathological examination results in the first trimester and second trimester was compared and analyzed for the pregnant women in two groups, and it was found that the ultrasound examination results in the second trimester were closer to the postpartum examination results, and the comparison was statistically great ($P < 0.05$), as illustrated in Figure 6.

4. Discussion

CNSM is a main factor leading to fetal stillbirth or death after delivery, and it has been studied by medical experts [10]. Early screening of CNSM is very important. The main inspection method is ultrasound, which can provide a reasonable basis for the prenatal diagnosis of CNSM [11, 12]. With the enhancement of ultrasound technology and the improvement of equipment in recent years, the accuracy of fetal CNSM ultrasound diagnosis has become higher and higher. It has been recognized as the first choice for fetal CNSM screening, but there are still some limiting factors [10]. Researchers have used ultrasound to detect and diagnose 645 cases of CNSM fetuses; it is found that ultrasound misdiagnosis and missed diagnosis sometimes occur during the process due to the interference of factors such as the position of the fetus in the mother's body, the amount of amniotic fluid in the uterus, and the processing experience of ultrasound [11]. The results in this study revealed that the ultrasound diagnosis in the second trimester is more accurate than the first trimester. Previous research results have shown that the most feasible period for the examination of the fetal shape and fetal structure is the second trimester, which could display the fetal central nervous system and its growth and development more clearly, showing the significance of ultrasound in clinical scan of fetal CNSM [12, 13]. In addition, some other studies have proposed that the growth and development status of the fetus in the mother can be displayed using ultrasound imaging technology, which can be evaluated according to the intensity difference of the signal displayed in the image. In the early stage of pregnancy (17~19 weeks), the fetus can be scanned for malformations, and good results have been obtained, indicating that CNSM can be performed on the fetus in advance [14, 15].

In this study, the DLNN algorithm was adopted to build a model to optimize the ultrasound image so as to inspect the CNSM. As a result, it was found that compared with the conventional ultrasound inspection, the results of the proposed inspection method were better. Nowadays, deep learning has been widely used in various fields with the great development of artificial intelligence. The working principle of deep learning is mainly to use the deep neural network models to analyze and

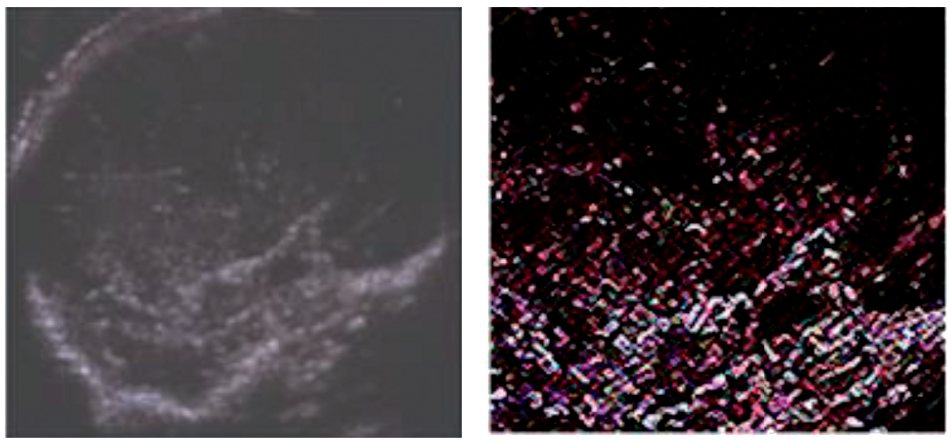

(a) (b)

Figure 2: Comparison of coronal section of fetal brain before and after processing of the ultrasound images: (a) experimental group; (b) control group.

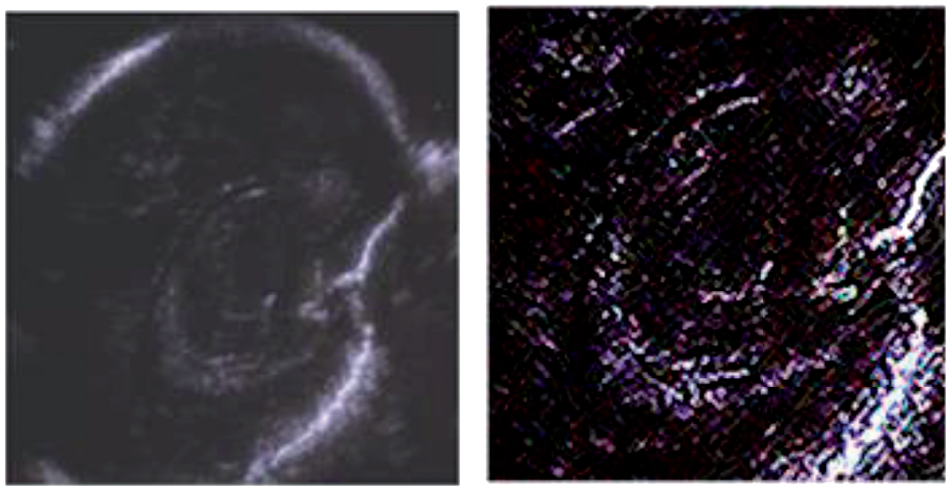

(a) (b)

Figure 3: Comparison of lateral ventricle parasagittal sectional ultrasound images before and after treatment of normal fetuses: (a) experimental group; (b) control group.

Table 2: Comparison between the prenatal and postpartum CNN-based ultrasound diagnosis results and the pathological biopsy results.

Type	Prenatal ultrasound results		Postpartum ultrasound and pathological results (case)
	Control group (case)	Experimental group (case)	
Coelosomia	16	18	20
Encephalocele	1	1	2
Rachischisis	9	10	12
Holoprosencephaly	3	5	5
Agenesis of corpus callosum	0	2	2
Hydrocephalus only	6	9	12
Anencephaly	5	6	8
Cerebellar dysplasia	0	1	2
Total	40	52	63

study the data and to improve the efficiency through feature extraction and feature classification [16, 17] so that more important application value can be reflected in the processing of medical images. Moreover, the public medical image database [18] and the medical image challenge data set [19] have enabled the deep learning methods to be well trained and verified in medicine, and the results obtained are more and more effective, so they have been widely recognized and

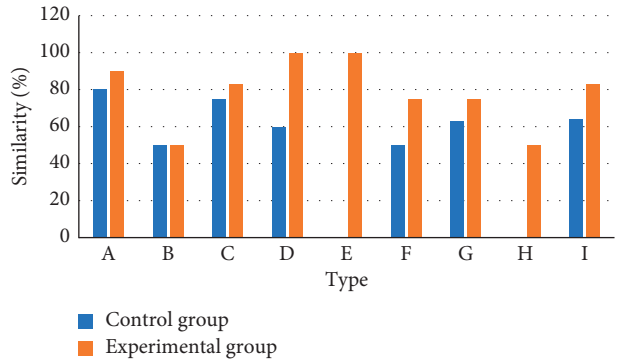

Figure 4: Comparison between the prenatal and postpartum ultrasound diagnosis results and the pathological results in term of similarity. Note: A, B, C, D, E, F, G, H, and I refer to coelosomia, encephalocele, rachischisis, holoprosencephaly, agenesis of corpus callosum, hydrocephalus only, anencephaly, and cerebellar dysplasia, respectively. *indicates a statistically significant difference, $P < 0.05$.

Table 3: Comparison of prenatal and postnatal ultrasound and pathological examination results at different pregnancy stages.

Type	The first trimester (17~19 weeks)		Second trimester (20~33 weeks)		Postnatal (case)
	Control group (case)	Experimental group (case)	Control group (case)	Experimental group (case)	
Coelosomia	9	15	16	18	20
Encephalocele	0	**0**	1	1	2
Rachischisis	3	8	9	10	12
Holoprosencephaly	2	4	3	5	5
Agenesis of corpus callosum	0	1	0	2	2
Hydrocephalus only	4	7	6	9	12
Anencephaly	3	5	5	6	8
Cerebellar dysplasia	0	0	0	1	2
Total	**21**	**40**	**40**	**52**	**63**

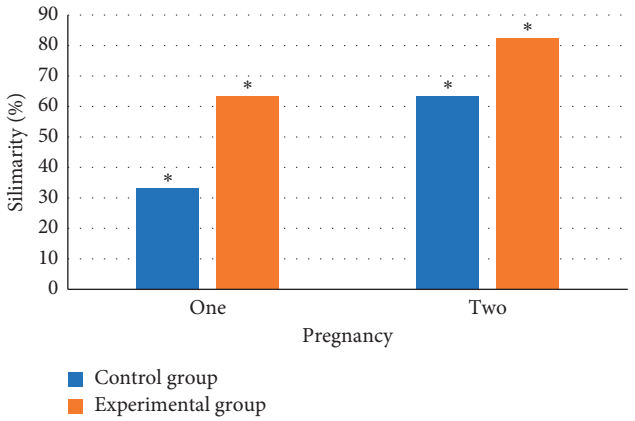

Figure 5: Comparison of the similarity of ultrasound examination results in different pregnancy stages between the two groups. Note: "one" and "two" refer to the first trimester and the second trimester, respectively. *indicates a statistically significant difference, $P < 0.05$.

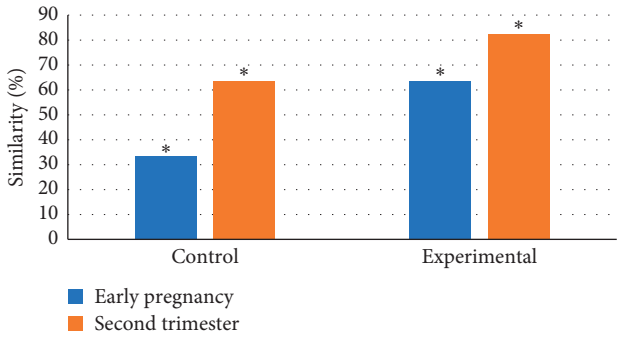

Figure 6: Comparison of the similarity of ultrasound examination results in different pregnancy stages in the two groups. *indicates a statistically significant difference, $P < 0.05$.

researched. Some experts have used the breast and fundus of the patient as the research subjects to study the application of CNN technology in processing medical images. They used CNN to segment the image and correct it. The result was verified on the public database e-ophtha EX database to prove the effectiveness of this method [20]. There was also a study on carotid artery ultrasound image plaque recognition using deep learning, where FasterRCNN based on VGG16 and ResNet101 and YOLOv3 based on Darknet were used. The results found that Faster RCNN was fast and accurate in plaque recognition of ultrasound images for carotid artery and should be suggested in clinic [21]. Gao et al. [22] applied the migration learning model of learning using privileged information (LUPI) in CNN to correct the intermediate state of network learning and also proposed a data generation strategy to maintain training samples; and the causal relationship with the privileged information in the label improved the insufficient medical data. Based on the above, it was concluded that the application of

deep learning in ultrasound inspection had very good development prospects.

5. Conclusion

In this study, the DLNN algorithm was adopted to identify and optimize the ultrasound examination images and applied to the screening of fetal CNSM. The statistical analysis of the examination result data revealed that the ultrasound image examination results of the experimental group were better than those of the control group, which meant that the ultrasound image based on deep learning had higher application value in CNSM examination. Moreover, the trend of the results of ultrasound images at different pregnancy stages was basically the same in the two groups, both of which showed that the effect of the experimental group was better. However, the results of different pregnancy stages for pregnant women in the experimental group suggested that the proposed method did not reduce the difference in the results at different pregnancy stages, indicating that the ultrasound technology needed to be improved further for examinations at different pregnancy stages so as to improve the accuracy of the examination results. The amount of data in this study was too small, so it was not representative, and there were still some shortcomings to be improved.

Data Availability

No data were used to support this study.

Conflicts of Interest

The author declares that there are no conflicts of interest.

References

[1] J. Gaitanis and T. Tarui, "Nervous system malformations," *Child Neurology*, vol. 24, no. 1, pp. 72–95, 2018.

[2] L. Manganaro, S. Bernardo, A. Antonelli, V. Vinci, M. Saldari, and C. Catalano, "Fetal MRI of the central nervous system: state-of-the-art," *European Journal of Radiology*, vol. 93, pp. 273–283, 2017.

[3] J. Yan, C. Zhou, F. Ye, and C. Gu, "RETRACTED: diagnosis of fatal central nervous system malformations based on prenatal colour doppler ultrasound," *Neuroscience Letters*, vol. 733, Article ID 135140, 2020.

[4] M. Yang, Y. Jiang, Q. Chen, M. Lv, and Q. Luo, "Prenatal diagnosis and prognosis of isolated subependymal cysts: a retrospective cohort study," *Prenatal Diagnosis*, vol. 37, no. 13, pp. 1322–1326, 2017.

[5] N. Zhang, H. Dong, P. Wang, Z. Wang, Y. Wang, and Z. Guo, "The value of obstetric ultrasound in screening fetal nervous system malformation," *World Neurosurgery*, vol. 138, pp. 645–653, 2020.

[6] H.-P. Chan, R. K. Samala, L. M. Hadjiiski, and C. Zhou, "Deep learning in medical image analysis," *Advances in Experimental Medicine & Biology*, vol. 1213, pp. 3–21, 2020.

[7] S. M. Anwar, M. Majid, A. Qayyum, M. Awais, M. Alnowami, and M. K. Khan, "Medical image analysis using convolutional neural networks: a review," *Journal of Medical Systems*, vol. 42, no. 11, p. 226, 2018.

[8] A. Savchenko, "Probabilistic neural network with complex exponential activation functions in image recognition," *IEEE Transactions on Neural Networks and Learning Systems*, vol. 31, no. 2, pp. 651–660, 2020.

[9] S. Shafique and S. Tehsin, "Acute lymphoblastic leukemia detection and classification of its subtypes using pretrained deep convolutional neural networks," *Technology in Cancer Research and Treatment*, vol. 17, Article ID 153303381880278, 2018.

[10] C. C. Morton, A. Metcalfe, K. Yusuf, B. Sibbald, and R. D. Wilson, "The impact of prenatal diagnosis of selected central nervous system Anomalies for prenatal counselling based on significant pregnancy morbidity and neonatal outcomes," *Journal of Obstetrics and Gynaecology Canada*, vol. 41, no. 2, pp. 166–173, 2019.

[11] Y. Melcer, R. Maymon, K. Krajden Haratz et al., "Termination of pregnancy due to fetal central nervous system abnormalities performed after 24 weeks' gestation: survey of 57 fetuses from a single medical center," *Archives of Gynecology and Obstetrics*, vol. 298, no. 3, pp. 551–559, 2018.

[12] I. B. Van den Veyver, "Prenatally diagnosed developmental abnormalities of the central nervous system and genetic syndromes: a practical review," *Prenatal Diagnosis*, vol. 39, no. 9, pp. 666–678, 2019.

[13] L. Edwards and L. Hui, "First and second trimester screening for fetal structural anomalies," *Seminars in Fetal and Neonatal Medicine*, vol. 23, no. 2, pp. 102–111, 2018.

[14] E. F. M. Santana, E. Araujo Júnior, E. Araujo Júnior, G. Tonni, F. Da Silva Costa, and S. Meagher, "Acrania-exencephaly-anencephaly sequence phenotypic characterization using two- and three-dimensional ultrasound between 11 and 13 weeks and 6 days of gestation," *Journal of Ultrasonography*, vol. 18, no. 74, pp. 240–246, 2018.

[15] W. Sepulveda, F. De La Maza, and S. Meagher, "An unusual first-trimester ultrasound presentation of the aanencephaly sequence," *Journal of Ultrasound in Medicine*, vol. 39, no. 4, pp. 829–832, 2020.

[16] T. Ching, D. S. Himmelstein, B. K. Beaulieu-Jones et al., "Opportunities and obstacles for deep learning in biology and medicine," *Journal of The Royal Society Interface*, vol. 15, no. 141, Article ID 20170387, 2018.

[17] Y. Chen, S. Hu, H. Mao, W. Deng, and X. Gao, "Application of the best evacuation model of deep learning in the design of public structures," *Image and Vision Computing*, vol. 102, no. 2020, Article ID 103975, 2020.

[18] L. K. Tan, R. A. McLaughlin, E. Lim, Y. F. Abdul Aziz, and Y. M. Liew, "Fully automated segmentation of the left ventricle in cine cardiac MRI using neural network regression," *Journal of Magnetic Resonance Imaging*, vol. 48, no. 1, pp. 140–152, 2018.

[19] G. Litjens, T. Kooi, B. E. Bejnordi et al., "A survey on deep learning in medical image analysis," *Medical Image Analysis*, vol. 42, pp. 60–88, 2017.

[20] F.-P. An and Z.-W. Liu, "Medical image segmentation algorithm based on feedback mechanism CNN," *Contrast Media and Molecular Imaging*, vol. 2019, Article ID 6134942, 13 pages, 2019.

[21] S. Savaş, N. Topaloğlu, Ö. Kazcı, and P. N. Koşar, "Classification of carotid artery intima media thickness ultrasound images with deep learning," *Journal of Medical Systems*, vol. 43, no. 8, p. 273, 2019.

[22] Z. Gao, S. Wu, Z. Liu et al., "Learning the implicit strain reconstruction in ultrasound elastography using privileged information," *Medical Image Analysis*, vol. 58, Article ID 101534, 2019.